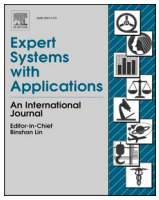
Expert Systems With Applications 293 (2025) 128675



Contents lists available at ScienceDirect

Expert Systems With Applications

journal homepage: www.elsevier.com/locate/eswa



Semantic-Preserved Generative Adversarial Network optimized with Tyrannosaurus Optimization Algorithm for Liver Disorder Classification

T. Haritha [a,*], A.V. Santhosh Babu [b]

[a] Assistant Professor, Department of Information Technology, Vivekanandha College of Engineering for Women, Tiruchengode, Namakkal - 637205, Tamil Nadu, India
[b] Professor, Department of Information Technology, Hindusthan Institute of Technology, Coimbatore-641032, Tamil Nadu, India

ARTICLE INFO

Keywords:
Distributed Set-Membership Fusion Filtering
Semantic-Preserved Generative Adversarial Network
Tyrannosaurus Optimization Algorithm

ABSTRACT

Liver disease causes around two million deaths annually, accounting for 4% of global deaths. The use of algorithms for early disease prediction in large clinical datasets shows promise, but is often constrained by the complexity and variability of the data. Therefore, Semantic-Preserved Generative Adversarial Network optimized using Tyrannosaurus Optimization Algorithm for Liver Disorder Classification (SPGAN-TOA-LDC) is proposed in this paper. Input data is collected from Indian Liver Patient Dataset (ILPD). The gathered data is fed into preprocessing stage using Distributed Set-Membership Fusion Filtering (DSMFF) to remove data redundancy. Hiking Optimization Algorithm (HOA) is employed to select the optimal features from the dataset. The selected features are supplied to Semantic-Preserved Generative Adversarial Network (SPGAN) to classify the liver disorder as liver disease and non-liver disease. Generally, SPGAN does not show any adaption of maximization approaches for identify the optimal parameters to ensure precise categorization of liver disorders. Tyrannosaurus Optimization Algorithm (TOA) is used for improving the weight parameters of SPGAN. The proposed SPGAN-TOA-LDC approach achieves 20.58%, 18.73% and 25.62% high accuracy, 24.58%, 28.73% and 15.62% high precision compared with existing techniques: CNN along machine learning models under Extra Trees Classifier with MRMR feature selection for liver disease identification on cloud (CNN-ILPD-LDC), Early identification of liver disease utilizing hybrid soft computing methods for optimum feature selection with categorization (DNN-ILPD-EDL), Liver disease patients prediction depending on integrated projection base statistical feature extraction and machine learning approaches (KNN-ILPD-LDC) respectively.

1. Introduction

Nowadays, a million people suffer from liver disease every year. General liver problems include cirrhosis of the liver, hepatitis A, B, C, liver cancer. In 2017, liver cirrhosis claimed the lives of around 1.32 million people worldwide with males making up 66.7 % of these deaths and women 33.3 %. Advances in cutting-edge treatment and leading a healthy lifestyle are lowering mortality (Terlapu et al., 2021). In this century, liver illness has been responsible for 3.5 % of deaths. The primary causes of liver disease like excessive drug and alcohol use, obesity, diabetes. The liver is the most commonly affected organ because it is the longest organ in the body. Hepatitis, cirrhosis, fatty liver, liver cancer, chronic liver diseases are some types of liver illnesses (Varchagall and Adaguru Yogegowda, 2023). Amongst these, cirrhosis is the last stage deadly disease that decreases the survival rate of people (Shaheen et al., 2023). Liver is the largest fleshy organ in human body that disposes of harmful chemicals, increases metabolism and detoxifies the body (Choubey et al., 2023). Purifying blood and facilitating its flow to other areas of the body is the primary function (Mathew et al., 2024). It produces proteins to help blood coagulation (Singh et al., 2021). The improved images created are used to differentiate malignant and normal liver using computer-aided diagnosis. A problem with several real-world datasets that include information on liver disease detection is class imbalance. K-Nearest Neighbour (KNN) classifier performs poorly on the unbalanced database, because they treat neighbours evenly. The fuzzy KNN's weighted version addresses the problem of data imbalance by assigning a maximal weight to the neighbour of minority class data and a comparatively minimal weight to the neighbour of majority class data (Kumar and Thakur, 2021). Finding useful information in large medical datasets is a significant part of automated disease detection. Convolutional Neural Network (CNN) dependent method is employed for liver disease identification. The proficiency of CNN is compared with

* Corresponding author.
E-mail addresses: kalaiarasi.prakash@gmail.com (T. Haritha), santhosh.vadivalagan@gmail.com (A.V.S. Babu).

https://doi.org/10.1016/j.eswa.2025.128675
Received 12 November 2024; Received in revised form 5 May 2025; Accepted 17 June 2025
Available online 18 June 2025
0957-4174/© 2025 Elsevier Ltd. All rights are reserved, including those for text and data mining, AI training, and similar technologies.

traditional KNN, Naive Bayes (NB), Support Vector Machine (SVM). The ultrasound is the preferred modality because of its non-invasive, economical, and real-time imaging capabilities. The main objective is to predict liver illnesses utilizing modified fast region-dependent CNN based hybrid grasshopper tunicate swarm (Antony Asir Daniel and Jeha, 2023). By using correction network module under encoder-decoder structure and an enhanced Cycle-Generative Adversarial Network (GAN) for higher quality liver clinical production that includes a new loss function (Raja et al., 2024), the superiority of the created liver clinical imageries is considerably enhanced, shows contrasting and clear features (Shaban, 2024). A unique anatomy preserving generative adversarial network (ApGAN) is developed for creating simulated intra-operative ultrasound (Sim-iUS) of the liver using exact configuration information from pMR (Chen et al., 2024). First, the bimodal fusion depending on low-rank factors is proposed with an emphasis on useful data for hepatic parenchyma (Chen et al., 2023). A multi-level GAN is presented to improve the computed tomographic (CT) scans (Khan et al., 2023).

Many existing methods for manual liver disease classification are quite time-consuming and involve a tedious process that results in poorer accuracy and inter-expert variability (Dar et al., 2023). The use of automatic classification for heterogeneous diseases has expanded, which has a significant impact on the area of clinical medicine by relieving doctors of the laborious task of manually delineating diseases. The application of deep learning strategies can lessen the defines related to machine learning, show promise in resolving the limitations of conventional ML approaches to the categorization of liver disease. These shortcomings have motivated to do this work.

This study focuses on Semantic-Preserved GAN (SPGAN) for liver disorder classification, which preserves important semantic features and improves classification accuracy between liver disease and non-liver disease while GANs are widely used in various domains. HOA is used for optimal feature selection and lowering the dimensionality of dataset while focusing on the most useful characteristics. This method not only simplifies the model, but also improves its capacity to produce accurate classifications by utilizing the most important data attributes.

Major contributions of this research work are:

- SPGAN optimized with TOA for liver disorder classification (SPGAN-TOA-LDC) is proposed.
- DSMFF approach is utilized in the preprocessing phase to remove data redundancy for ensuring that the classification dataset is clean and free of repeating information, hence enhancing the overall accuracy and efficiency of the method.
- HOA is utilized for optimal feature selection, which aids in finding the dataset most relevant features for liver disorder categorization. HOA improves the classification model's performance by lowering dimensionality and focusing on most relevant information.
- SPGAN categorizes the liver problems into liver disease and non-liver disease groups. This uses the datasets semantic structure to ensure that relevant features are preserved, resulting in improved generalization and classification performance.
- TOA enhance the weight parameters of the SPGAN. It improves the networks performance by fine-tuning the parameters for better classification accuracy, ensuring that SPGAN categorizes liver illnesses more precisely.

Continuing paper is organized as: section II defines literature survey, section III describes materials and procedures, section IV proves outcomes and discussion and section V gives conclusion.

2. Literature survey

Several researches were based on deep learning dependent liver diseases detection and classification; some of recent researches are revised below,

Amin et al., (2023) presented patients with chronic liver disease estimation using machine learning approaches for integrated projection-dependent statistical feature extraction. Maximum variation in the data, covariance among observed variables and linear consolidation of observed variables that maximises class separation were used by the system for creating an enhanced feature space. The data balancing was done to avert bias with overfitting. The statistical models manage missing values and outliers. It attains greater precision and lesser specificity.

Varchagall and Adaguru Yogegowda, (2023) presented early recognition of liver infections under hybrid soft computing methods for ideal feature selection with categorization. Liver illness was primary causes of death and challenging to diagnose in its early stages. Unambiguous verification of inherent and characteristic elements was critical for developing new models for identifying and removing risk. Create a modified whale search optimisation (MWSO) method for the best feature selection, which integrates features that might represent the scattered semantic backdrop and texture patterns in the data. It has low specificity and low ROC.

Lanjewar et al., (2023) presented CNN and machine learning methods for cloud-based liver infection detection utilizing Extra Trees Classifier with MRMR feature selection. Every year, almost two million individuals suffered from liver illness and hundreds of millions more suffer from chronic liver disease. Liver illness was a major global health burden. MRI visual evaluation and liver biopsy were used to identify the subjects. It was a tedious and time-consuming procedure. It has maximal sensitivity, but minimal f-score.

Krishnamurthy et al., (2021) introduced particle swarm optimization for the categorization of liver disease ultrasound imageries using multiple level and multiple domain variables. Using ultrasound scans to classify liver illnesses presents a number of obstacles at every stage, starting with classification. When a broad subset of liver illnesses was used strong features and the best possible combinations of classification parameters were required to achieve a respectable level of classification accuracy. Using the particle swarm optimisation technique, an optimisation problem was formulated to minimise the fivefold cross validation error to categorize ten different kinds of disorders. It has high precision and less sensitivity.

Singh and Agarwal, (2023) introduced extreme learning machines for liver disease analysis and prediction. The human analysis was a laborious and time-consuming procedure and the development of a fully autonomous computer-assisted disease prediction model was a great assistance to medical practitioners. An automated mode for liver disease prediction using extreme learning machine classifier that uses the user's biological traits was introduced. It has maximal precision, but more computation time.

Yasmin et al., (2023) presented designing of new feature union to predict liver illness patients: machine learning method. To remove duplicate information from the data, ML researchers frequently utilise feature selection and feature extraction algorithms separately. However, relying solely on one approach could not provide the expected performance or outcomes. The dataset of liver disease patients from India should was used when implementing the recommended technique to categorize liver disease utilizing machine learning classifiers. It has greater accuracy and lesser ROC.

Gupta et al., (2022) introduced liver disease prediction utilizing machine learning categorization techniques. The liver patient data collection obtained from UCI Repository was presented. Many patient records were available from hospital physicals. Information on liver patients has been taken from these records and utilised to treat their illnesses in the future. It attains high precision and less ROC.

3. Proposed Methodology

In this paper, SPGAN-TOA-LDC is proposed. The input images are taken from Indian Liver Patient Dataset (https://www.kaggle.com/data

sets/uciml/indian-liver-patient-records). The gathered images are pre-processed by using DSMFF. The SPGAN does not adapt any optimization techniques for determining optimal parameters to ensure the precise categorization of liver disorders. So, TOA is proposed to enhance the SPGAN that classifies the liver disorder accurately. Fig. 1 represents block diagram of SPGAN-TOA-LDC method.

3.1. Dataset description

Indian Liver Patient Dataset (ILPD) (Wu et al., 2023) comprises 583 patient records gathered from hospitals in North East Andhra Pradesh, India, as well as 416 liver illness, 167 non-liver illness cases. This database comprises 441 male together with 142 female patients, with any patient above 89 years old listed as 90 for standardization. It comprises ten biochemical and demographic characteristics that are essential for liver disease detection, including age, gender, total bilirubin, direct bilirubin, alkaline phosphatase, alanine aminotransferase, aspartate aminotransferase, total proteins, albumin, and the albumin-globulin ratio. The dataset column is goal variable, identifying patients as liver disorder present or not. The patient class distribution bar diagram is represented in Fig. 2.

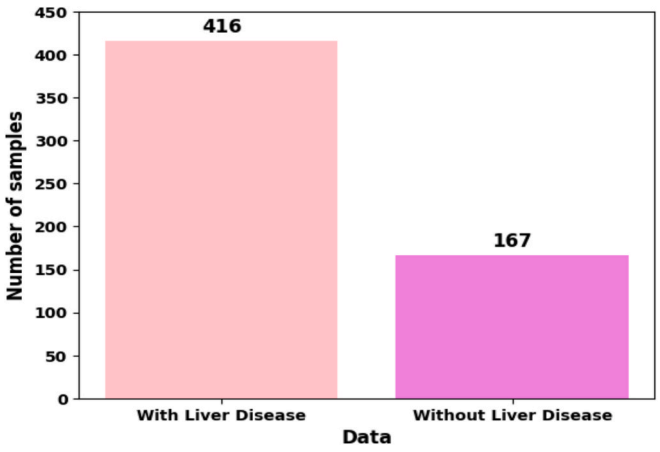


Fig. 2. Patients class distribution bar diagram.

3.2. Preprocessing under distributed Set-Membership fusion filtering

DSMFF (Wu et al., 2023) is used to remove data redundancy in liver disease categorization, because it provides an efficient and robust technique to dealing with unclear and duplicated data in medical datasets. DSMFF operates on a set-membership foundation as opposed to traditional filtering approaches, such as Kalman filtering or Particle filtering which rely on probabilistic assumptions and have computational inefficiencies while processing huge amounts of medical data. This makes it ideal for applications in which accurate probability distributions are unavailable. Furthermore, classic data fusion techniques such as weighted averaging or Bayesian fusion fail to adjust dynamically to changes in redundant data, but DSMFF effectively manages such changes by applying real-time set-based restrictions. The set membership filter for the nonlinear distributed encoding–decoding system built for the nonlinear two-dimensional shift changing system expressed in Eq. (1),

$$\hat{y}_{m,s} = \hat{y}_{s|s-1} + Q_{m,s}\left(h_{m,s} - Q_{m,s^{\hat{y}_{s|s-1}}}\right) \tag{1}$$

here $\hat{y}_{m,s}$ denotes local estimate of m, s on sensor r, $Q_{m,s^{\hat{y}_{s|s-1}}}$ denotes filter parameters. DSMFF eliminates data redundancy by employing an adaptive constraint-based filtering process that compares each data point to a predetermined membership set before including it in the final dataset. It uses set-membership constraints to keep just the most relevant and non-redundant data points, ensuring that duplicate measurements are removed. The linearized formula is expressed in Eq. (2),

$$Q_{m,s} = \hat{L}_{s|s-1} Z^{E}_{m,s}\left(\frac{Z_{m,s}\hat{L}_{s}}{1-\partial_{m,s}} + \frac{S_{m,s}}{\partial_{m,s}}\right) \tag{2}$$

Nonlinear functions $\partial_{m,s}$ of Taylor series expansion formula are linearized. This is important in liver condition classification, when numerous data modalities tests yield overlapping data. By integrating these limitations into a distributed framework, DSMFF assures that data from different sources are fused appropriately while ensuring consistency and avoiding redundant information. The high order Lagrange remainders is given in Eq. (3),

$$\hat{L}_{m,s} = \frac{\hat{L}_{s|s-1}}{1-\partial_{m,s}}\left(1 - \frac{Q_{m,s}Z_{m,s}}{1-\partial_{m,s}}\right) \tag{3}$$

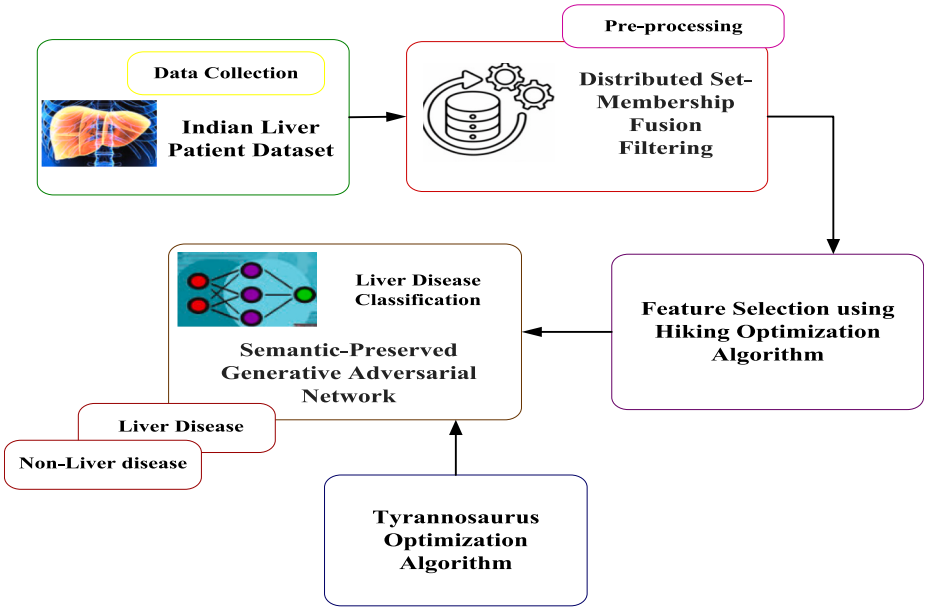


Fig. 1. Block diagram of SPGAN-TOA-LDC method.

here $\widehat{L}_{m,s}$ implies Jacobian matrices, $Q_{m,s}Z_{m,s}$ signifies high orders Lagrange remainders. This not only increases the classification model's computing efficiency, but also improves its accuracy and generalizability by ensuring that training data is diverse and representative, rather than biased by duplicate. Ideal value of $\partial_{m,s}$ is expressed in Eq. (4),

$$\partial m, s = \frac{\sqrt{\delta_n}}{\sqrt{\delta_n + \sqrt{s_n}}} \tag{4}$$

here δ_n and s_n signifies maximum singular values of matrices $\partial m, s$. To identify s cluster using iteration lessens loss function. Node m removes ellipsoidal center data, wherein loss function is definite as sum of distance error square. DSMFF is utilized to eliminate data redundancy formulated in Eq. (5),

$$I\,(d,\,\eta)\;=\;\sum_{j=1}^{N}\|y_j-\eta_s\|^2 \tag{5}$$

here y_j signifies I sample, $d,\ \eta$ represents centroid connected to cluster, N signifies count of ellipsoidal centers or shapes. The pre-processing output is given towards feature extraction procedure.

3.3. Feature selection using Hiking optimization Algorithm

Hiking Optimization Algorithm (HOA) (Oladejo et al., 2024) is discussed for feature selection process. HOA was inspired by the hikers proficiencies who were trying to reach the top of mountains, hills or rocks. Hikers can consciously or unconsciously assess the steepness of the terrain when they are trekking. They stay away from really steep trails and terrain to keep up their walking or trekking pace. This can take longer to find the worldwide optimum that is akin to what happens to hikers during a trip. The approach is based on the idea of tackling optimisation problems by simulating the experience of hiking.

Step 1: Initialization

The population in HOA has to be initialized through creating a randomwise solutions collection. It can use the following matrix to indicate that each Hiking Optimization procedure is expressed in Eq. (6),

$$D=\begin{bmatrix} D_1^1 & D_1^2 & \ldots & \ldots & D_1^b \\ D_2^1 & D_2^2 & \ldots & \ldots & D_2^b \\ \ldots & \ldots & \ldots & \ldots & \ldots \\ \ldots & \ldots & \ldots & \ldots & \ldots \\ D_n^1 & D_n^2 & \ldots & \ldots & D_n^b \end{bmatrix} \tag{6}$$

where D represents total hiker, n represents the amount of trails, and b is the execution decision variables.

Step 2: Random generation

Generate the input parameters at random from initialization. Optimal fitness value is selected depends on explicit hyperparameter situation.

Step 3: Fitness function

It creates random solution through initialization. The HOA approach is used to assess the fitness of all position vector that corresponds to every data. This is computed by Eq. (7),

$$\textit{Fitness Function}\;=\;\textit{Selecting}\;\;[\,\textit{optimal features}\,] \tag{7}$$

Step 4: Compute the Initial Hiking Velocity and Slope

Tobler's Hiking Function (THF) accounts for route or terrain slope and steepness when calculating a hiker's speed. It is exhibited in Eq. (8),

$$\vartheta_{a,t}=6e^{-3.5\left|l_{a,t}+0.05\right|} \tag{8}$$

here, $l_{a,t}$ is trail's or terrain's slope and $\vartheta_{a,t}$ implies hiker's a velocity (km/h) at iteration or time t.

Step 5: Determine the absolute velocity of Hiker.

HOA takes advantage of both the collective social cognition of hikers and each hiker's unique cognitive capacities. The lead hiker's position, the hiker's real position, the sweep factor and the beginning velocity ascertained by THF all contribute to update or real velocity of hiker. The hiker a's current velocity is measured by Eq. (9),

$$\vartheta_{a,t}=\vartheta_{a,t-1}+\delta_{a,t}\left(\lambda_{best}-\varsigma_{a,t}\lambda_{a,t}\right), \tag{9}$$

here the variable $\delta_{a,t}$ represents uniformly distributed count at interval [0, 1]; the current and beginning velocities of hiker a are indicated by $\vartheta_{a,t}$ and $\vartheta_{a,t-1}$, respectively. The lead hiker position denotes λ_{best}, the hiker sweep factor (SF) denotes $\varsigma_{a,t}$, which is located in [1, 3].

Step 6: Update the Hikers position

The SF follows the lead hiker's path, listens to their signals, and ensures that the hiker not wander away from them. Consider the hiker's velocity in (20), hiker a's revised position $\lambda_{a,t+1}$ is articulated in Eq. (10),

$$\lambda_{a,t+1}=\lambda_{a,t}+V_{a,t} \tag{10}$$

where upper bound ϕ_b^2 and lower bound ϕ_b^1 of the solutions, which dictate the initialisation of hiker locations $\lambda_{a,t}$.

Step 7: Termination

HOA is used for selecting the optimum feature, otherwise, step 3 repeats iteratively until fulfil halting condition. The selected features like age, sex, total bilirubin, direct bilirubin, alanine amino transferase, total proteins and albumin-globulin ratio are supplied as input to the classification.

3.4. Liver disorder classification under Semantic-Preserved Generative adversarial Network

Liver disorder categorization using SPGAN (Li et al., 2023) is discussed. Semantic-preserved GANs maintain the meaning and coherence of generated data, ensuring high-quality synthetic outputs. The SPGAN classifier generates its final predictions through the discriminator after modifying its final sigmoid into a softmax layer for liver disease and non-liver disease classification. During adversarial training SPGAN implements semantic consistency loss to create synthetic samples that maintain vital clinical patterns while addressing class imbalance issues. The semantically guided augmentation processes better than conventional methods, as it generates authentic and varied samples. And SPGAN achieves dual optimization by using adversarial training to match synthetic data distributions with real liver-disorder imagery and semantic preservation to maintain feature integrity. The dual optimization goal of SPGAN improves convergence speed and reduces false positive errors because standard methods lack any convergence criteria. Medical validity and semantic richness in generated samples by the SPGAN enables better model generalization and reduces overfitting compared to traditional methods.

The knowledge transferability in actual and synthetic datasets for semantic feature preservation is given using Eq. (11),

$$P_{GAN}\left(F,G,C_R,C_E,J_R,J_E\right)\;=\;T_{y_e\sim}Y_E[\log C_E(y_e)\,] \tag{11}$$

Apply a similar image-consistency constraint to inspire the preservation of the source content during the conversion process. Cycle consistency is enforced by reproducing the original sample by mapping it source to target and back to source in equation (12),

$$P_{imgf}(F,G,J_R,J_E)=T_{yr\sim}Y_R\left[\|G_{img}(y_r)-y_r\|_1\,\right] \tag{12}$$

where P_{imgf} stands for $\ell 1$ normal GNA-basis source-domain-target-domain picture translation deems 2 mentioned losses, it rising to bias. The imageries produced by the generator is nearer in distribution to the target specified in equation (13),

$$P_{rep}(F, G, J_R, J_E) = T_{y_r} \sim Y_R[\|F_{enc}(y_s) - G_{enc}\|] \quad (13)$$

The semantic constraints can be introduced during the training process in an elegant and efficient manner with this approach, which no need any pre-trained modes at the source domain is represented in equation (14),

$$P_{sem}(F, J_R) = T_{(y_r, x_r)\sim(Y_R, X_R)}[p(F_{sem}(y_r), x_r)] \quad (14)$$

here P_{sem} implies cross-entropy loss function,y_r implicates source domain label, P_{sem} denotes probability. The entire loss function of SPGAN is labelled in equation (15),

$$P_{SPGAN} = P_{GAN}\begin{pmatrix} F, G, C_R, \\ C_E, J_R, J_E \end{pmatrix} + \gamma_1 P_{ing}(F, G, J_R, J_E) \quad (15)$$

where γ_1 set to γ_2 set to 1, γ_3 is gradually large along the training epochs. The labeled translated image G and unlabeled target image J_R; P_{ing} symbolize selection indicator for randomly chosen half classes pixel in $J_{R,}$; C_E if the pixel, located at the $J_{E,}$ column belonging to the designated classes P_{GAN}.

Fig. 3 depicts the SPGAN-DA framework, which consists of two major stages: (1) semantic-preserving source to target transformation, (2) class distribution arrangement for semantic segmentation. The first stage involves a Cycle GAN-like architecture that translates imageries from source to target domain, while maintaining semantic structures. This is accomplished using two generators: $G : E \rightarrow R$ The generator F encodes the source image using F_{enc}, extracts segmentation-related features via F_{seg} and reconstructs the translated target data through F_{dec} ensuring semantic preservation through semantic loss, adversarial loss as well as image consistency loss,G reconstructs the source data from target domain using *enc* and *dec* functions. In the second stage, the translated and mixed data are input into a semantic segmentation network for collaborative training, which aligns class distributions across domains. The segmentation network is trained with cross-entropy loss for labels and boundary (BD) loss for edges, resulting in accurate segmentation in the target domain while reducing domain shift. The general goal of creating data adaptation boundary improvement identified liver disease and non-liver illness based on the aforementioned factors is shown in Eq. (16),

$$P_{total} = P_{seg} + \gamma_a \cdot (P_{src_a} + P_{mix_a}) \quad (16)$$

Let γ_a represents hyper-parameter for controlling the weight of boundary enhancement component. Finally, the SPGAN classified liver and non-liver disease. The SPGAN classifier considers artificial intelligence-dependent optimization method because of its pertinence. TOA is considered to optimize the SPGAN parameter P *and* Y and tune the weight with bias factor of SPGAN.

3.5. Optimization utilizing Tyrannosaurus optimization Algorithm

The weights parameter P *and* Y of SPGAN is enhanced by TOA (Sahu et al., 2023). The TOA improves SPGAN for liver disorder classification by utilizing an adaptive exploration–exploitation balance, resulting in diversified and high-quality feature learning while avoiding mode collapse. It efficiently optimizes hyperparameters, improves feature selection and handles skewed and noisy data, hence increasing model robustness. TOA's parallel search algorithms speed convergence while lowering processing costs and increasing real-time applicability. Their enhanced global search capability allows it to avoid local minima, resulting in better generalization, higher classification accuracy and greater stability than traditional optimizers. Optimizing Tyrannosaurusrex (T-Rex) hunting involves adjusting speed and success rate parameters to assess their impact on prey capture. Prey can defend itself by making different speed escapes after the prey running speediness operator is introduced. The estimation rate (ER) operator determines hunting success or failure. TOA solve these problems effectively.

3.5.1. Step-by-step process of TOA

The stepwise process is defined to optimize the image to determine the optimal share for the retrieval of image using TOA. TOA makes evenly distributing populace the optimization of lifetime dependability, implementation time and power consume from the task-scheduling scheme. The optimal solution is provoked by TOA and associated flowchart is depicted in Fig. 4.

Step 1: Initialization

A number of prey is generated randomly in the search space through the population-dependent technique known as TOA. Let Y represent the location or position of the prey, which is random wise generated in the search area between the higher and lower bounds shown in Eq. (17),

$$Y_j = sand(ml, \dim) * (va - pa) + pa \quad (17)$$

here $(ml, \dim)$ is the prey location, m denotes dimension, pa denotes

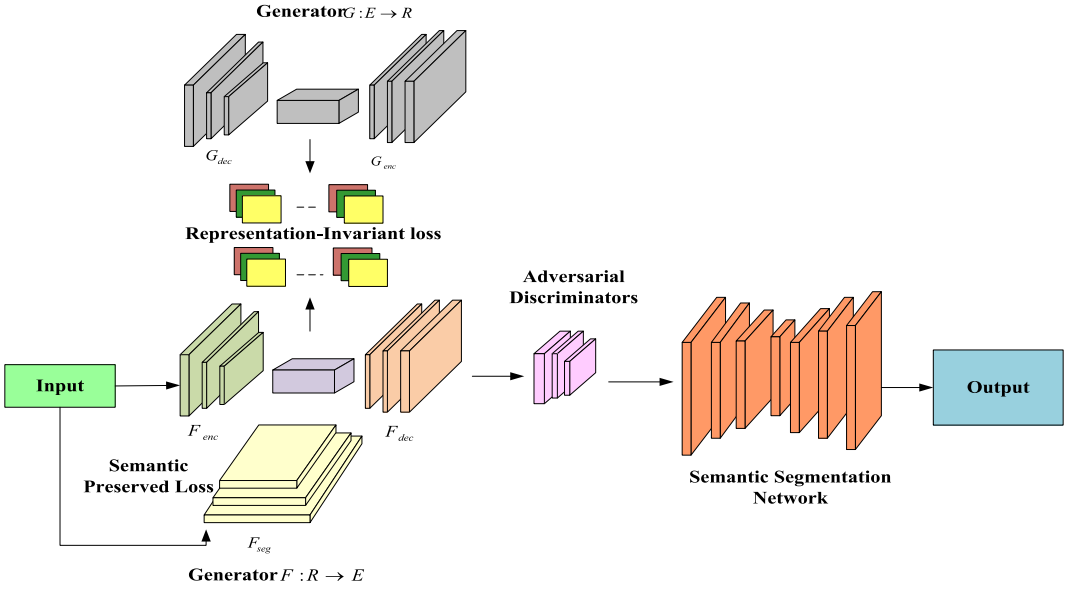


Fig. 3. Architecture diagram of Semantic-Preserved Generative Adversarial Network.

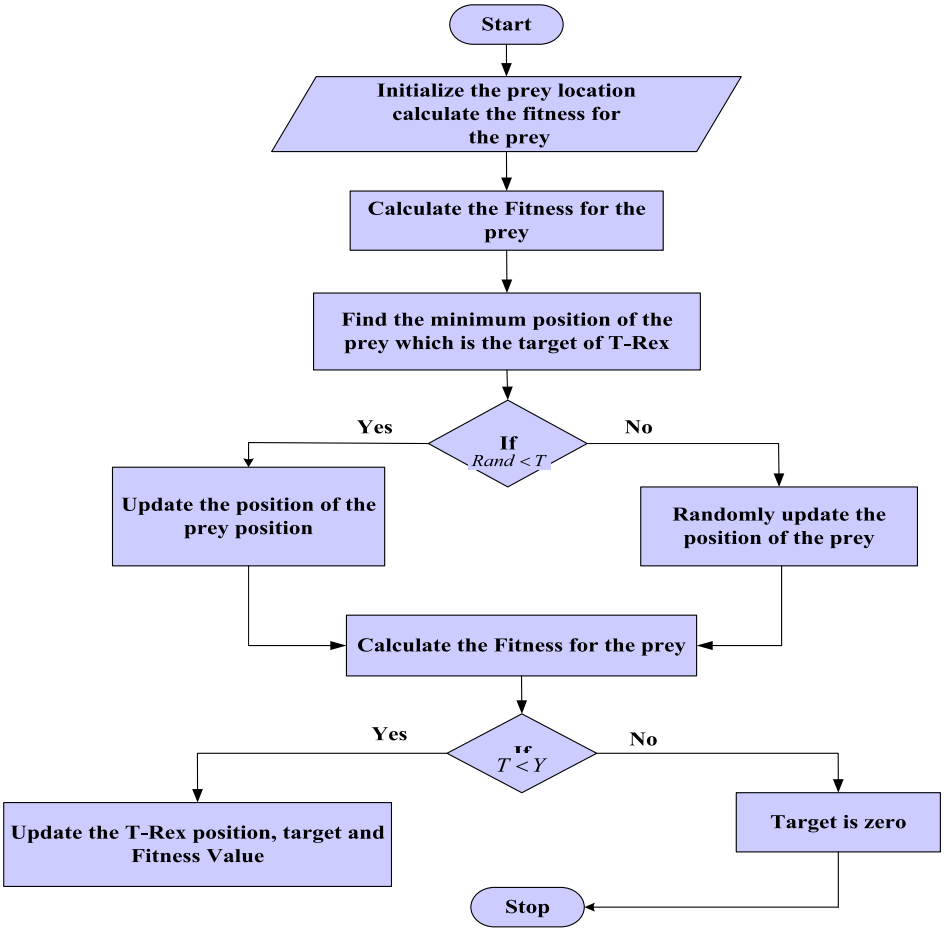


Fig. 4. Flowchart of TOA to optimize SPGAN parameter.

count of populace, dim specifies dimension of search space, *va* specifies upper limit.

Step 2: Random generation

Create the input parameters randomly after initialization. Optimum fitness values are selected using clear hyperparameter circumstance.

Step 3: Fitness function evaluation

Random solution is generated from initialization. This is evaluated with parameter optimization to enhance weight parameter *P and Y* classifier by Eq. (18),

$$fitness\ function = optimizing\ \ (P\ and\ Y) \tag{18}$$

Step 4: Hunting and chasing

T-Rex chases their prey like wolf, lion. T-Rex tries for hunting the target that is very close to it. A prey occasionally defends itself from predators or able to escape and it hunts at random in Eq. (19),

$$Y_{new} = \begin{Bmatrix} y_{new} & if\ rand() < Ts \\ Random & else \end{Bmatrix} \tag{19}$$

here *Ts* implies assessment of achieving the scattered prey. The prey begins to break apart as soon as the T-Rex begins hunting, and it chases the prey through update its location using Eq. (20),

$$y_{new} = y + rand * rs * (epos * es - target * ls) \tag{20}$$

where, *es* denotes success rate for hunting lies amongst [0.1,1]. If the hunt failed, the prey escaped, success rate is 0 and prey positioning is updated. The target is where located the prey in relation to the T-Rex.

Step 5: Exploitation to optimize *P and Y*.

The prey location, intended prey current location and prey past location plays a vital role in the selection process. The prey position becomes zero if the T-Rex does not hunt and it flees or defends from predators. This is recognized by analysing the fitness function is shown in Eq. (21),

$$y_j^{q+1} = \begin{Bmatrix} P < Y \\ target\ is\ zero \end{Bmatrix} \tag{21}$$

here *P* implies fitness function for the initial random prey location, *Y* implies fitness function to update prey position.

Step 6: Termination

The weight factor for generator *P and Y* of SPGAN is enhanced using TOA; else iterative repeat step 3 until the halting criteria $Y = Y+1$ is satisfied. Finally, SPGAN-TOA-LDC identifies liver disease and non-liver disease with better accuracy by decreasing computational time without error.

4. Result and discussion

The experimental outputs of the SPGAN-TOA-LDC technique are deliberated in this section. The SPGAN-TOA-LDC is simulated in Python utilizing workstation equipped with 11-GEN CPU, Intel Core i7 along 8 GB RAM (Vishwanatha et al.,2023). The acquired results of the proposed SPGAN-TOA-LDC method is compared to the existing CNN-ILPD-LDC (Amin et al., 2023), DNN-ILPD-EDL (Varchagall and Adagur-uYogegowda, 2023), KNN-ILPD-LDC (Lanjewar et al., 2022). Table 1 tabulates the simulation parameter.

Table 1
Simulation Parameter.

Parameter	Values
Learning Rate	0.0002
Batch Size	32
Number of Epoch	100
Loss Function	Binary Cross-Entropy (BCE) + MSE Loss
Generator Layers	4 Conv Layers + BatchNorm + ReLU
Discriminator Layers	4 Conv Layers + LeakyReLU + Dropout
Population Size	50
Number of Iterations	100
Dropout Rate	0.5
Regularization	L2 Regularization ($\lambda = 0.0001 - 0.001$)
Selection Mechanism	Fitness-Based Selection
Crossover Probability	0.8
Convergence Criterion	Threshold-Based Improvement

4.1. Performance measures

Measurement of classification performance is necessary to determine whether the given classification algorithm operates satisfactorily or not. The following confusion matrixes are needed to evaluate the performance measures.

- True Negative (TN): negative values accurately characterized as negative.
- True Positive (TP): positive values accurately characterized as positive.
- False Positive (FP): positive values inaccurately characterized as negative.
- False Negative (FN): negative values inaccurately characterized as positive

4.1.1. Accuracy

The ratio of correctly categorized cases to total cases in the database is calculated using Eq. (22),

$$Accuracy = \frac{(TP + TN)}{(TP + FP + TN + FN)} \tag{22}$$

4.1.2. Precision

It computes true positive prediction rate relative to sum of true as well as false positive predictions by Eq. (23),

$$Precision = \frac{TP}{(TP + FP)} \tag{23}$$

4.1.3Sensitivity

It scales the ratio of positive rates that are successfully classified through the prediction model using Eq. (24),

$$sensitivity = \frac{TP_a}{(TP_a + FN_T)} \tag{24}$$

4.1.3. F-score

It combines precision and recall in a single value and provide a balanced estimation using Eq. (25),

$$F1 - Score = 2 \times \frac{recall \times precision}{recall + precision} \tag{25}$$

4.1.4. Specificity

This is defined as true negative rate. It is the percentage of liver diseases correctly classified by the model using Eq. (26),

$$\text{Specificity} = \frac{TN}{(FP + TN)} \tag{26}$$

4.1.5. ROC

ROC provides information about liver disorder in advanced IoT and is calculated through Eq. (27),

$$ROC = 0.5 \times \left(\frac{TP}{TP + FN} + \frac{TN}{TN + TP}\right) \tag{27}$$

4.2. Performance analysis

Figs. 5-11 portrays performance analysis of SPGAN-TOA-LDC method. The effectiveness of the SPGAN-TOA-LDC is compared with existing methods.

Fig. 5 specifies accuracy evaluation. Accuracy is evaluating the presentation of SPGAN. The optimized SPGAN improves the model's learning potential by maintaining important semantic properties while producing synthetic liver ailment data. It assures that the method accurately generalizes to previously unseen data, lowering misclassification rates and contributes to a high accuracy score. The proposed SPGAN-TOA-LDC achieves 20.58 %, 18.73 %, 25.62 %high accuracy for liver disease; 30.51 %, 27.96 %, 22.29 % high accuracy for non-liver disease compared with existing methods.

Fig. 6 depicts precision estimation. Precision is high because SPGAN-TOA successfully distinguishes between liver disorder and non-disorder cases. The feature selection and semantic preservation algorithms ensure that the classifier learns fine-grained details while reducing the amount of false positives. The proposed SPGAN-TOA-LDC achieves 24.58 %, 28.73 %, 15.62 % greater precision for liver disease; 20.44 %, 22.96 %, 24.29 % higher precision for non-liver disease compared with existing methods.

Fig. 7 represents sensitivity analysis. SPGAN-TOA has great sensitivity because it detects liver disorders effectively in complex or borderline cases. The GAN-based data augmentation aids in dealing with minority class difficulties, ensuring that the method is well-trained in a wide range of liver condition data. The proposed SPGAN-TOA-LDC approach achieves 26.78 %, 15.47 %, and 22.67 % greater sensitivity for liver disease; 22.73 %, 21.42 % and 19.79 % better accuracy for non-liver disease compared with existing methods.

Fig. 8 shows f-score analysis. This is high because precision and recall are evenly balanced. SPGAN provides high-quality synthetic samples that improve class distribution while avoiding data imbalance difficulties. The proposed SPGAN-TOA-LDC achieves 21.18 %, 23.72 %, 17.67 % greater f-score for liver disease analysis; 20.68 %, 21.80 % and 24.69 % greater f-score for non-liver disease than existing methods.

Fig. 9 depicts specificity analysis. The model's high specificity stems from its ability to accurately remove healthy cases from being misclassified as ill. This lowers the false positive rate and enhances specificity. The proposed SPGAN-TOA-LDC method attains 20.58 %, 19.73 % and 23.62 %higher specificity for liver disease; 28.54 %, 27.77 % and 15.29 % higher specificity for non-liver disease compared with existing methods.

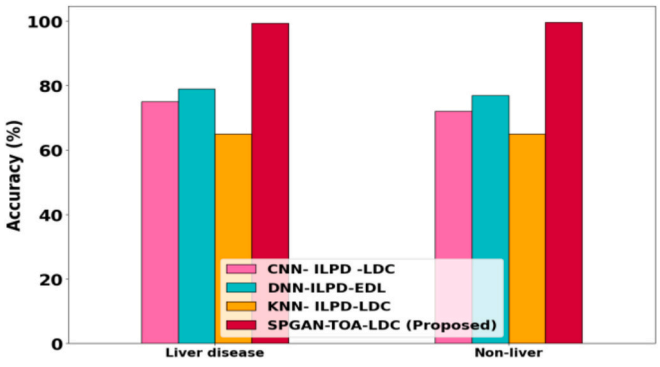


Fig. 5. Accuracy analysis.

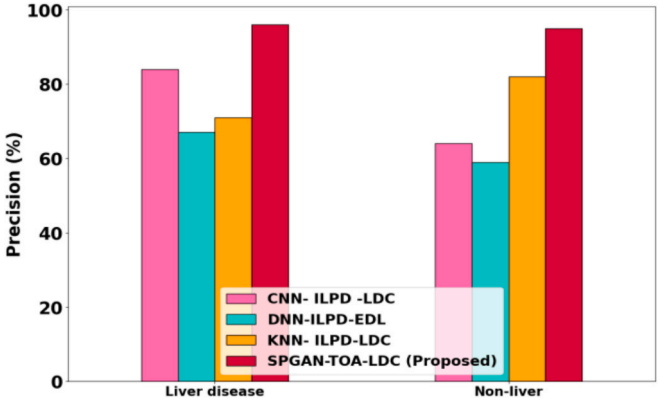


Fig. 6. Precision analysis.

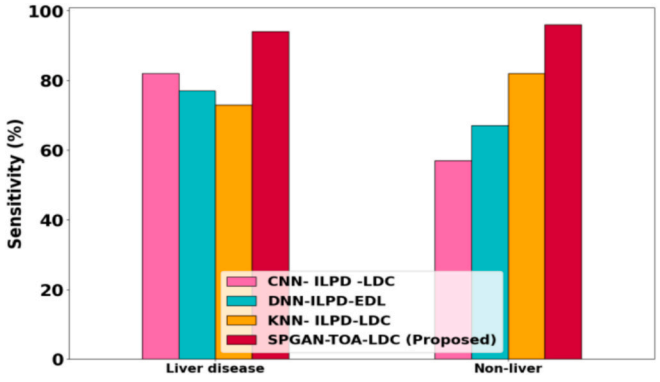


Fig. 7. Sensitivity analysis.

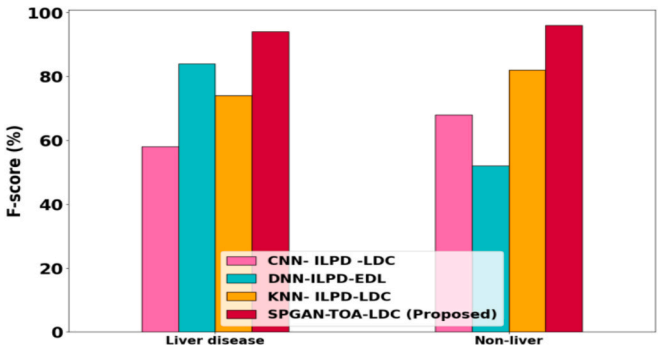


Fig. 8. F-score analysis.

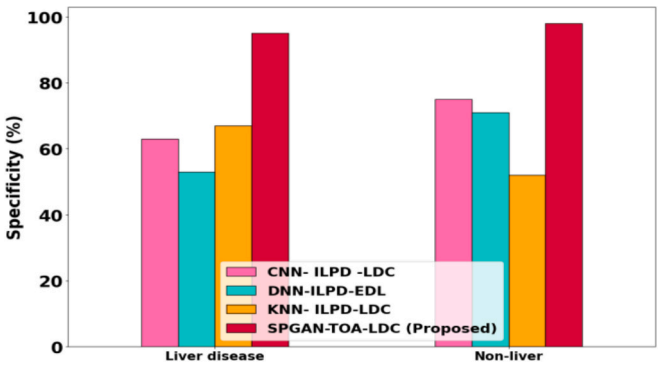


Fig. 9. Specificity analysis.

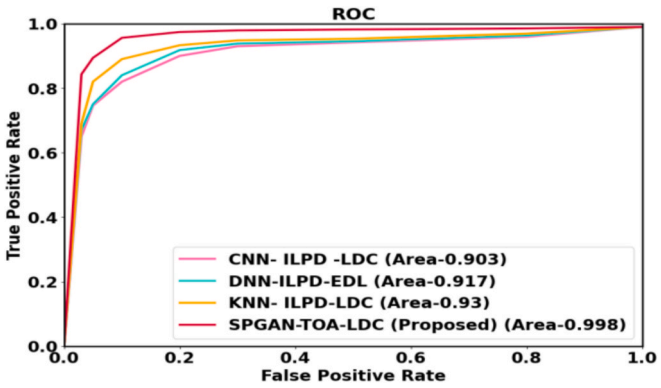


Fig. 10. ROC analysis.

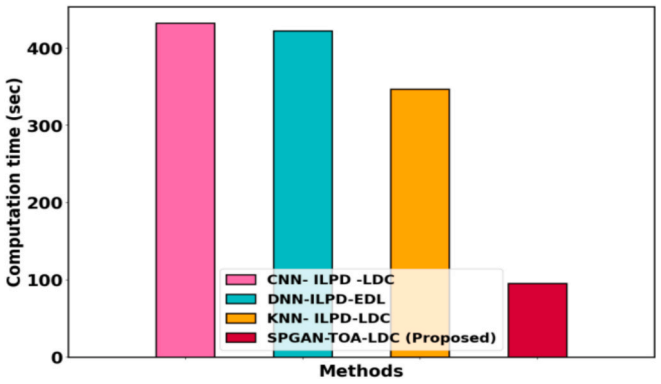


Fig. 11. Computational time analysis.

Fig. 10 shows ROC estimation. SPGAN boosts the techniques capability to discriminate among liver disorder, non-disorder instances by creating realistic synthetic samples that improve decision bounds. As a result, the ROC is large, showing that the classifier performs well across a range of threshold values, assuring reliable classification performance. Thresholds for the ROC curve in the SPGAN optimized with the TOA are determined to balance sensitivity and specificity while maximizing the ROC. Cross-validation and domain-specific factors are used in the procedure, with the goal of reducing false negatives in medical contexts. The proposed SPGAN-TOA-LDC achieves 32.30 %, 30.92 %, 27.37 % high ROC compared with existing methods.

Fig. 11 depicts computational time analysis. Computational time is reduced due to TOA's efficient hyperparameter tuning and SPGAN's ability to generate high-quality, representative synthetic data. The algorithm ensures that the model converges faster and with fewer iterations by eliminating redundant features and maximizing learning rates. Despite the intricacy of the model, the overall computational cost is acceptable, making the proposed method suitable for real-world applications. The SPGAN-TOA-LDC attains 280 s, 250 s and 240 s less

Table 2
Performance analysis of computational efficiency metrics.

Performance analysis	Methods			
	CNN-ILPD-LDC	DNN-ILPD-EDL	KNN-ILPD-LDC	SPGAN-TOA-LDC (proposed)
Memory consumption (GB)	5.4	4.3	4.8	3.2
Inference Time (ms)	23	34	20	12
Power consumption (Wh)	156	148	116	95

computational time compared with existing models.

Table 2 shows the performance analysis of computational efficiency metrics. When compared to baseline approaches, the proposed SPGAN-TOA-LDC method outperforms them in terms of computational efficiency. It has the lowest memory consumption of 3.2 GB, considerably lowering resource utilization. The inference time of 12 ms is the fastest, allowing for real-time forecasts with minimal latency. Furthermore, power consumption of 95 Wh is the lowest, resulting in increased energy efficiency. These findings demonstrate the efficiency of optimization algorithms role in lowering computing costs while retaining good performance.

Table 3 compares the performance of proposed and existing methods and shows their 95 % confidence intervals for accuracy, precision, sensitivity, f-score, specificity. The confidence intervals show the range within which genuine performance numbers are predicted to fall with 95 % certainty. The DNN-ILPD-EDL exhibited the best accuracy of 99.47 % but somewhat worse precision and recall than others. KNN-ILPD-LDC provided balanced performance with high specificity of 98.20 %, whereas SPGAN-TOA-LDC performed competitively across all parameters. The tight confidence intervals of ± 0.09 indicate strong dependability and consistency for the stated performance results.

Table 4 compares classification performance across five dimensions as accuracy, precision, sensitivity and ROC. The accuracy stays high across all folds, with an average of 99.12 %, suggesting great overall performance. Precision of 98.32 % indicates less false positive rate, and sensitivity of 96.68 % demonstrates the method's capacity to detect true positives. The ROC is 0.97, indicating excellent class discrimination. Variations between folds imply model robustness with occasional swings in Sensitivity, presumably due to data distribution variations. The model operates well and is highly reliable.

Table 5 presents a comparative analysis of four data augmentation methods evaluated on key metrics. SPGAN delivers the most effective results through its 15.2 FID score, 0.89 diversity level, 5.1 % false positives and 50 epoch convergence speed. SPGAN outperforms both Synthetic Minority Over-sampling Technique (SMOTE) (Elreedy et al., 2024) and Adaptive Synthetic Sampling (ADASYN) (Elshaboury et al., 2024) since it creates semantically meaningful and realistic samples through its generation process. The performance of Vanilla GAN (Bisht et al., 2024) is moderate yet it does not achieve the semantic consistency that SPGAN provides. SPGAN delivers exceptional data augmentation through its ability to create meaningful clinical data which improves classification accuracy while minimizing errors and training time.

Table 6 presents the cross-dataset generalization performance of the proposed SPGAN–TOA–LDC model. The model displayed better generalization output when trained on ILPD data and evaluated on BUPA data resulting in 97.80 % accuracy and 0.98 AUC. The BUPA → ILPD evaluation yielded 96.50 % accuracy with 0.97 AUC score. The technique demonstrated greater accuracy of 97.50 % when tested using ILPD → SPGAN synthetic data and the model demonstrates effective generalization capabilities while preventing overfitting based on the results presented for both real and synthetic datasets. The ILPD self-test achieved the best accuracy rate at 99.63 % which indicates optimal within-distribution performance.

Table 3
Performance analysis of proposed SPGAN-TOA-LDC.

Performance metrics	Methods			
	CNN-ILPD-LDC	DNN-ILPD-EDL	KNN-ILPD-LDC	SPGAN-TOA-LDC (proposed)
Accuracy (95 % CI)	99.14 ± 0.09	99.47 ± 0.09	99.38 ± 0.09	99.63 ± 0.09
Precision (95 % CI)	96.74 ± 0.09	96.17 ± 0.09	96.83 ± 0.09	96.97 ± 0.09
Sensitivity (95 % CI)	98.97 ± 0.09	96.69 ± 0.09	96.25 ± 0.09	96.43 ± 0.09
F-score (95 % CI)	98.69 ± 0.09	96.11 ± 0.09	98.25 ± 0.09	97.24 ± 0.09
Specificity (95 % CI)	97.30 ± 0.09	97.55 ± 0.09	98.20 ± 0.09	98.34 ± 0.09

Table 4
K-fold validation results.

Fold	Accuracy (%)	Precision (%)	Sensitivity (%)	ROC
1	99.1	97.85	97.45	0.98
2	99.6	98.10	96.18	0.99
3	99.5	98.32	97.75	0.97
4	98.10	99.24	96.40	0.97
5	99.30	98.10	95.62	0.96
Average	99.12	98.32	96.68	0.97

Table 5
Comparative Analysis of Augmentation Methods.

Augmentation Method	FID Score	Diversity Score	False Positives (%)	Epochs to Converge
Vanilla GAN	20.5	0.82	9.8	60
SMOTE	28.7	0.72	17.3	80
ADASYN	26.5	0.70	16.0	85
SPGAN (proposed)	15.2	0.89	5.1	50

Table 6
Cross–Dataset Generalization Results.

Train → Test	Accuracy	Precision	Sensitivity	Specificity	AUC
ILPD → BUPA	97.80 %	96.75 %	96.45 %	97.10 %	0.98
BUPA → ILPD	96.50 %	96.31 %	96.80 %	96.90 %	0.97
ILPD → SPGAN Synthetic	97.50 %	97.10 %	97.00 %	97.50 %	0.98
SPGAN Synthetic → ILPD	96.90 %	96.50 %	96.31 %	96.70 %	0.97
ILPD (self–test)	99.63 %	98.92 %	98.27 %	98.14 %	0.99

4.3. Computational complexity analysis

Tyrannosaurus Optimization Algorithm like other metaheuristic optimization techniques has a computational complexity primarily influenced by a count of iterations I and population size M. The time complexity per iteration depends on the cost function evaluation and the search mechanism, typically requiring $O(M.h(d))$ operations, where $h(d)$ represents the complexity of evaluating the fitness functions, d is the dimensional search space. The proposed method follows a global exploration and local exploitation strategy, leading to an overall complexity of $O(I.N.h(d))$.

Fig. 12 portrays computational complexity evaluation. The graph

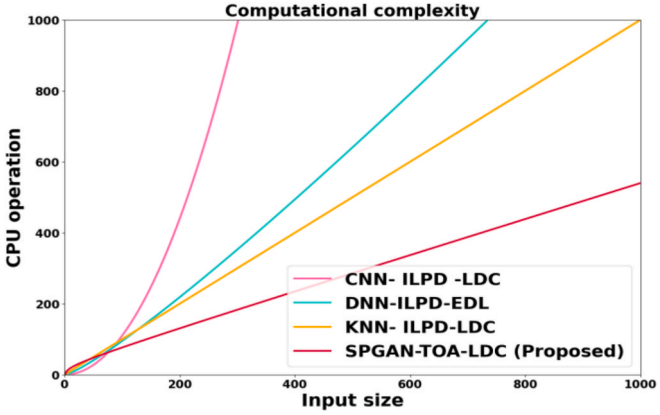


Fig. 12. Computational complexity analysis.

analyzes the computational complexity under CPU processes along input size. The SPGAN-TOA-LDC achieves less time complexity, shows better proficiency than other models, this become gradually problematic as raises the input size. It proves the scalability of SPGAN-TOA-LDC.

4.4. GAN training dynamics

Fig. 13 shows Generator vs. Discriminator Loss Curve and it illustrates the training dynamics of SPGAN by plotting generator and discriminator loss curves over 100 iterations and the combined plot shows that both discriminators loss and generators loss start from high initial values before reaching a stable plateau at iteration 40. The training process shows no sudden spikes or oscillations because both networks avoid mode collapse and gradient vanishing. The discriminator achieves faster convergence than the generator because its loss values remain consistently lower than those of the generator which indicates its ability to detect real from synthetic samples. The steady decline of loss values during training demonstrates balanced adversarial training and validates the effectiveness of gradient clipping and batch normalization methods. The experimental results show that SPGAN maintains stable convergence together with semantic consistency throughout the process.

4.5. Ablation study

Table 7 shows the ablation study and importance of all components of SPGAN-TOA-LDC framework.

The ablation study examines the effects of several components on model performance. Removing DSMFF reduces accuracy of 96.56 % and sensitivity of 94.15 %, demonstrating its importance in feature extraction. Excluding HOA significantly reduces sensitivity of 96.78 %, demonstrating its importance in optimization. Without TOA, sensitivity increases of 98.56 %, but accuracy decreases of 95.78 %, indicating that TOA helps balance performance. The proposed SPGAN-TOA-LDC model attains the greatest 99.16 % accuracy and 99.14 % F-score, demonstrating its ability to improve the efficacy of overall prediction.

4.6. Statistical analysis

Table 8 exhibits ANOVA to compute the performance variations mid-different approaches by analyzing the other models. The analysis exemplifies variations amongst between and within the models to accepting SPGAN-TOA-LDC effectiveness.

The ANOVA Table 8 assesses the statistical significance of differences in classification models for liver condition identification. The Sum of Squares (SS) quantifies the variation, with Between Groups SS of 450.23 representing variance caused by different models and Within Groups SS of 920.45 showing individual differences within each model. The F-Value of 8.76 reflects the ratio of inter-group to intra-group variation, while the P-Value of 0.0021 validates statistical significance of $P < 0.05$, indicating that one model outperforms others. This validates the efficiency of the SPGAN, which is optimized with the TOA for liver disorder categorization.

4.7. Discussion

The proposed SPGAN-TOA-LDC offers a novel and cutting-edge method for the early liver diseases identification to address the urgent need for precise classification in healthcare. This model utilises a wide range of SPGAN and integrates them across the diagnostic techniques. The data preprocessing using DSMFF is used to remove redundant information from the ILPD. In the feature extraction process, the Quaternion offset linear canonical transform is used to extract important information from higher dimensions to lower dimensions. The experimental evaluation of the proposed SPGAN-TOA-LDC method demonstrates its superiority over existing techniques.

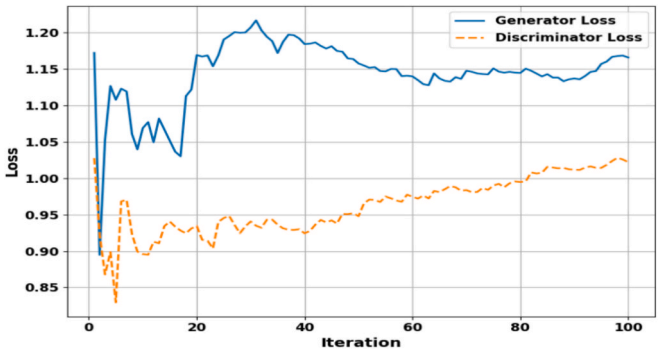


Fig. 13. Generator vs. Discriminator Loss Curve.

Table 7
Ablation Study.

Ablation Mode	Accuracy (%)	Precision (%)	sensitivity (%)	F-score (%)
Without DSMFF	96.56	95.14	94.15	93.67
Without HOA	97.12	96.23	96.78	95.17
Without TOA	95.78	97.12	98.56	97.23
SPGAN-TOA-LDC (proposed)	99.16	98.92	99.27	99.14

Table 8
ANOVA examination.

Source of Variation	SS	DF	MS	F-value	P-value
Between Methods	450.23	2	225.12	8.76	0.0021
Within Methods	920.45	37	24.87		
Total	1370.68	39			

The HOA consistently selected four features that directly match clinically accepted hepatic dysfunction biomarkers including total bilirubin, alanine aminotransferase (ALT), albumin–globulin ratio and alkaline phosphatase. The conjugation pathways become impaired when total bilirubin levels rise and ALT activity indicates hepatocellular damage. The albumin–globulin ratio demonstrates liver synthetic function and inflammatory state while elevated alkaline phosphatase indicates cholestasis. The selection of these features by HOA improves both model classification performance and maintains a connection to proven pathophysiological mechanisms which enhances clinical interpretability and practical application.

5. Conclusion

In this paper, SPGAN optimized with TOA for liver disorder classification was implemented successfully. The SPGAN-TOA-LDC achieves 79.68 %, 80.97 % and 76.36 % greater accuracy 30.10 %, 31.97 % and 29.86 % greater sensitivity and 28.48 %, 31.40 % and 32.46 % greater ROC compared with existing models.

Declaration of competing interest

The authors declare that they have no known competing financial interests or personal relationships that could have appeared to influence the work reported in this paper.

Data availability

No data was used for the research described in the article.

References

Amin, R., Yasmin, R., Ruhi, S., Rahman, M. H., & Reza, M. S. (2023). Prediction of chronic liver disease patients using integrated projection based statistical feature extraction with machine learning algorithms. *Informatics in Medicine Unlocked., 36*, Article 101155.

Antony Asir Daniel, V., & Jeha, J. (2023). An optimal modified faster region cnn model for diagnosis of liver diseases from ultrasound images. *IETE Journal of Research., 24*, 1–8.

A. Bisht K. Rawat J.P. Bhati S. Vats V. Sharma S. Singh November. generating images using Vanilla generative Adversarial networks In 2024 4th International Conference on Technological Advancements in Computational Sciences (ICTACS) 2024 (pp. 463–468).IEEE.

Chen, L., Liao, H., Kong, W., Zhang, D., & Chen, F. (2023). Anatomy preserving GAN for realistic simulation of intraoperative liver ultrasound images. *Computer Methods and Programs in Biomedicine., 1*(240), Article 107642.

Chen, Y., Lin, H., Zhang, W., Chen, W., Zhou, Z., Heidari, A. A., Chen, H., & Xu, G. (2024). ICycle-GAN: Improved cycle generative adversarial networks for liver medical image generation. *Biomedical Signal Processing and Control., 1*(92), Article 106100.

D.K. Choubey P. Dubey B.P. Tewari M. Ojha J. Kumar Prediction of liver disease using soft computing and data science approaches. In6G Enabled Fog Computing in IoT: Applications and Opportunities, 2 2023 Oct Springer Nature Switzerland Cham 183 213.

Dar, A. H., & Bhat, Y. M. (2023). Donoho-Stark's and Hardy's uncertainty principles for the short-time quaternion offset linear canonical transform. *Filomat., 37*(14), 4467–4480.

Elshaboury, N., Yamany, M. S., Labi, S., & Smadi, O. (2024). Enhancing local road pavement condition prediction using bayesian-optimized ensemble machine learning and adaptive synthetic sampling technique. *International Journal of Pavement Engineering., 25*(1), Article 2365957.

Elreedy, D., Atiya, A. F., & Kamalov, F. (2024). A theoretical distribution analysis of synthetic minority oversampling technique (SMOTE) for imbalanced learning. *Machine Learning., 113*(7), 4903–4923.

Gupta K, Jiwani N, Afreen N. Liver disease prediction using machine learning classification techniques. In 2022 IEEE 11th International conference on communication systems and network technologies (CSNT) 2022' Apr 23 (pp. 221-226).IEEE. https://www.kaggle.com/datasets/uciml/indian-liver-patient-records.

Khan, R. A., Luo, Y., & Wu, F. X. (2023). Multi-level GAN based enhanced CT scans for liver cancer diagnosis. *Biomedical Signal Processing and Control., 1*(81), Article 104450.

Krishnamurthy, R. K., Radhakrishnan, S., & Kattuva, M. A. (2021). Particle swarm optimization-based liver disorder ultrasound image classification using multi-level and multi-domain features. *International Journal of Imaging Systems and Technology., 31*(3), 1366–1385.

Kumar, P., & Thakur, R. S. (2021). Liver disorder detection using variable-neighbor weighted fuzzy K nearest neighbor approach. *Multimedia Tools and Applications., 80*, 16515–16535.

Lanjewar, M. G., Parab, J. S., Shaikh, A. Y., & Sequeira, M. (2023). CNN with machine learning approaches using ExtraTreesClassifier and MRMR feature selection techniques to detect liver diseases on cloud. *Cluster Computing., 26*(6), 3657–3672.

Li, Y., Shi, T., Zhang, Y., & Ma, J. (2023). SPGAN-DA: Semantic-preserved generative adversarial network for domain adaptive remote sensing image semantic segmentation. *IEEE Transactions on Geoscience and Remote Sensing*.

Mathew, M. G., Jeevanandan, G., Maganur, P. C., Tamah, A. A., Ayyashi, Y. A., Tawhari, A. I., & Vishwanathaiah, S. (2024). Evaluation of Risk Factors associated with Caries Development after Full-mouth Rehabilitation for Early Childhood Caries Under General Anesthesia. *The Journal of Contemporary Dental Practice, 25*(1), 85–91.

Oladejo, S. O., Ekwe, S. O., & Mirjalili, S. (2024). The hiking optimization algorithm: A novel human-based metaheuristic approach. *Knowledge-Based Systems., 19*(296), Article 111880.

Raja, G., Reka, K., Murugesan, P., & MeenakshiSundaram, S. (2024). Predicting liver Disorders using an extreme Learning machine. *SN Computer Science., 5*(6), 677.

Sahu, V. S., Samal, P., & Panigrahi, C. K. (2023). Tyrannosaurus optimization algorithm: A new nature-inspired meta-heuristic algorithm for solving optimal control problems. e-prime-advances in electrical engineering. *Electronics and Energy., 5*, Article 100243.

Shaban, W. M. (2024). Early diagnosis of liver disease using improved binary butterfly optimization and machine learning algorithms. *Multimedia Tools and Applications., 83*(10), 30867–30895.

Shaheen, H., Ravikumar, K., Anantha, N. L., Kumar, A. U., Jayapandian, N., & Kirubakaran, S. (2023). An efficient classification of cirrhosis liver disease using hybrid convolutional neural network-capsule network.biomedical signal processing and. *Control., 80*, Article 104152.

G. Singh A.C. Prediction analysis of liver disease using extreme learning machine. InSentiment Analysis and Deep Learning: Proceedings of ICSADL, 2023 jan 1 2022 Springer Nature Singapore Singapore 679 690.

Singh L, Janghel RR, Sahu SP. Classification of hepatic disease using machine learning algorithms.InAdvances in Biomedical Engineering and Technology: Select Proceedings of ICBEST 2018 2021 (pp. 161-173). Springer Singapore.

Terlapu, P. V., Sadi, R. P., Pondreti, R. K., & Tippana, C. R. (2021). Intelligent identification of liver diseases based on incremental hidden layer neurons ann model. international journal of computing and digital. *System.*

Varchagall, M., & AdaguruYogegowda, P. (2023). Early detection of liver disorders using hybrid soft computing techniques for optimal feature selection and classification. *Concurrency and Computation: Practice and Experience., 35*(6), 1.

Varchagall, M., & AdaguruYogegowda, P. (2023). Early detection of liver disorders using hybrid soft computing techniques for optimal feature selection and classification. *Concurrency and Computation: Practice and Experience., 35*(6), 1.

Vishwanatha CR, Asha V, Prasad A, Manoj SS, Kindalkar SN, Bhatt SR. Prediction of Liver Disease Using Machine Learning Algorithms. In2023 International Conference on Computational Intelligence for Information, Security and Communication Applications (CIISCA) 2023 Jun 22 (pp. 154-159). IEEE.

Wu, H., Zhu, H., Li, X., & Amuri, M. J. (2023). Trust-based distributed set-membership filtering for target tracking under network attacks. *IEEE Access*.

R. Yasmin R. Amin M.S. Reza Design of Novel Feature Union for Prediction of Liver Disease Patients: A Machine Learning Approach. In The Fourth Industrial Revolution and Beyond: Select Proceedings of IC4IR+, 3 2023 Jun Springer Nature Singapore Singapore 515 526.